Supplementary Information

Synthetic, Spectral, Structural and Catalytic activity of infinite 3-D and 2-D Copper(II) Coordination Polymers for Substrate Size-Dependent Catalysis for CO_2 Conversion

Bhaskaran,[a] Manoj Trivedi,[a*] Anita K. Yadav,[b] Gurmeet Singh,[a*] Abhinav Kumar,[c] Girijesh Kumar,[d] Ahmad Husain,[e] Nigam P. Rath[f**]

[a]Department of Chemistry, University of Delhi, Delhi-110007, INDIA.
[b]Department of Chemistry, Rajdhani College, University of Delhi, Delhi-110015, INDIA
[c]Department of Chemistry, University of Lucknow, Lucknow-206007, INDIA
[d]Department of Chemistry and Center of Advanced Studies in Chemistry, Panjab University, Chandigarh-160014, INDIA
[e]Department of Chemistry, DAV University, Jalandhar, Punjab, INDIA
[f]Department of Chemistry & Biochemistry and Centre for Nanoscience, University of Missouri-St. Louis, One University Boulevard, St. Louis, MO 63121-4499, USA.

Corresponding authors: E-mail address: manojtri@gmail (M.T.); rathn@umsl.edu(NPR); gurmeet123@gmail (G.S.). Tel.: + 91 9811730475 (MT); + 91 9810390640(G.S.); (314) 516-5333 (NPR).

Table 1. Crystallographic data for **1** and **2**.

Empirical Formula	$C_{11}H_{18}N_2O_8Cu_2$	$C_{34}H_{36}N_6O_8Cu$
FW	433.35	720.23
crystal system	Tetragonal	Monoclinic
space group	*P4₂/nnm*	*P2₁/c*
a, Å	10.8365(15)	16.4200(14)
b, Å	10.8365(15)	8.2055(7)
c, Å	13.6420(3)	12.2480(10)
α, deg	90	90
β, deg	90	110.921(3)
γ, deg	90	90
V, Å^3	1602.0(5)	1541.4(2)
Z	4	2
d_{calc}, g cm^{-3}	1.797	1.552
μ, mm^{-1}	2.696	0.775
T, K	293(2)	100(2)
R_1 all	0.0841	0.0604
R_1 [I > 2σ(I)]	0.0687	0.0413
wR_2	0.1788	0.1179
wR_2 [I > 2σ(I)]	0.1721	0.1071
GOF on F^2	1.234	1.046

[a]$R_1 = \Sigma||Fo| - |Fc||/\Sigma|Fo|$; $wR_2 = \{\Sigma[w(|Fo|2 - |Fc|2)2]/\Sigma[wFo,4]\}^{1/2}$.

Table 2. Selected bond lengths (Å), and bond angles (°) for **1** and **2**.

Compound 1		**Compound 2**	
Cu(1)-O(1)$^{\#1}$	1.945(5)	Cu(1)-O(1$^{\#1}$	1.9420(16)
Cu(1)-O(1)	1.945(5)	Cu(1)-O(1)	1.9420(16)
Cu(1)-O(2)$^{\#2}$	1.965(5)	Cu(1)-O(3)$^{\#2}$	1.9534(16)
Cu(1)-O(2)$^{\#3}$	1.965(5)	Cu(1)-O(3)$^{\#3}$	1.9535(16)
Cu(1)-N(1)	2.343(6)	O(1)-C(1)	1.279(3)
Cu(1)-Cu(1)$^{\#2}$	2.6317(19)	O(2)-C(1)	1.241(3)
O(1)-C(1)	1.249(8)	O(3)-C(8)	1.268(3)
O(2)-C(1)	1.265(8)	O(4)-C(8)	1.250(3)
O(2)-Cu(1)$^{\#2}$	1.965(5)	N(1)-C(9)	1.493(3)
N(1)-C(4)$^{\#4}$	1.477(5)	N(1)-C(12)	1.501(3)
N(1)-C(4)	1.477(5)	N(2)-C(13)	1.362(3)
N(1)-C(3)	1.479(9)	N(2)-C(11)	1.458(3)
C(1)-C(2)	1.499(9)	N(2)-C(10)	1.460(3)
C(3)-N(1)$^{\#5}$	1.479(9)	N(3)-C(17)	1.334(3)
C(4)-N(1)$^{\#6}$	1.477(5)	N(3)-C(13)	1.354(3)
O(1)$^{\#1}$-Cu(1)-O(1)	91.4(4)	O(1)$^{\#1}$-Cu(1)-O(1)	180.0
O(1)$^{\#1}$-Cu(1)-O(2)$^{\#2}$	87.4(2)	O(1)$^{\#1}$-Cu(1)-O(3)$^{\#2}$	86.98(7)
O(1)-Cu(1)-O(2)$^{\#2}$	168.0(2)	O(1)-Cu(1)-O(3)$^{\#2}$	93.02(7)
O(1)$^{\#1}$-Cu(1)-O(2)$^{\#3}$	168.0(2)	O(1)$^{\#1}$-Cu(1)-O(3)$^{\#3}$	93.02(7)
O(1)-Cu(1)-O(2)$^{\#3}$	87.4(2)	O(1)-Cu(1)-O(3)$^{\#3}$	86.98(7)
O(2)$^{\#2}$-Cu(1)-O(2)$^{\#3}$	91.2(3)	O(3)$^{\#2}$-Cu(1)-O(3)$^{\#3}$	180.0
O(1)$^{\#1}$-Cu(1)-N(1)	99.37(18)	C(1)-O(1)-Cu(1)	118.48(14)
O(1)-Cu(1)-N(1)	99.37(18)	C(8)-O(3)-Cu(1)#4	110.10(14)
O(2)$^{\#2}$-Cu(1)-N(1)	92.60(18)	O(2)-C(1)-O(1)	127.2(2)
O(2)$^{\#3}$-Cu(1)-N(1)	92.60(18)	O(2)-C(1)-C(2)	116.83(19)

$O(1)^{\#1}$-Cu(1)-$Cu(1)^{\#2}$	85.09(15)	O(1)-C(1)-C(2)	115.83(19)
$O(2)^{\#2}$-Cu(1)-$Cu(1)^{\#2}$	82.91(15)	O(4)-C(8)-O(3)	124.9(2)
N(1)-Cu(1)-$Cu(1)^{\#2}$	173.56(17)	O(4)-C(8)-C(3)	118.00(19)
C(1)-O(1)-Cu(1)	123.1(4)	O(3)-C(8)-C(3)	116.99(19)
C(1)-O(2)-$Cu(1)^{\#2}$	124.2(4)	C(9)-N(1)-C(12)	112.79(18)
C(4)-N(1)-Cu(1)	113.4(3)	C(13)-N(2)-C(11)	123.21(19)
C(3)-N(1)-Cu(1)	103.5(4)	C(13)-N(2)-C(10)	122.92(19)
O(1)-C(1)-O(2)	124.3(6)	C(11)-N(2)-C(10)	113.33(18)
O(1)-C(1)-C(2)	119.0(6)	C(17)-N(3)-C(13)	115.9(2)
O(2)-C(1)-C(2)	116.7(6)	N(1)-C(9)-C(10)	110.51(19)
N(1)-C(3)-$N(1)^{\#5}$	111.1(8)	N(2)-C(10)-C(9)	109.37(19)
N(1)-C(4)-$N(1)^{\#6}$	110.7(7)	N(2)-C(11)-C(12)	110.66(19)
		N(1)-C(12)-C(11)	111.56(19)
		N(3)-C(13)-N(2)	116.9(2)

Table 3. Hydrogen bond parameters for **1** and **2**.

D-H···A-X	*d* H···A Å	*D* D···A Å	*θ* D-H···Aº
Compound 1			
C(3)-H(3A)···O(2)[a]	2.52	3.112(8)	119
C(3)-H(3B)···O(2)[b]	2.52	3.112(8)	119
Symmetry transformations used to generate equivalent atoms: (a) -1+y,x,-z: -x,1-y,-z; (b)1/2-y,1/2-x,-z:-1/2+ x,-1/2+y,-z.			
Compound 2			
C(9)-H(9A)...O(1)[#1]	2.46	3.431(3)	167.4
C(11)-H(11A)...N(3)[#5]	2.63	3.514(3)	149.2
C(12)-H(12A)...O(1)[#4]	2.59	3.535(3)	158.7
C(12)-H(12B)...O(3)[#2]	2.27	3.130(3)	144.9
N(1)-H(1A)...O(4)[#4]	1.88(4)	2.761(3)	164(3)
N(1)-H(1B)...O(2)	1.80(3)	2.690(3)	168(3)
Symmetry transformations used to generate equivalent atoms: [#1] -x+1,-y+1,-z+1; [#2] -x+1,y-1/2,-z+1/2; [#3] x,-y+3/2,z+1/2; [#4] -x+1,y+1/2,-z+1/2; [#5] x,-y+3/2,z-1/2.			

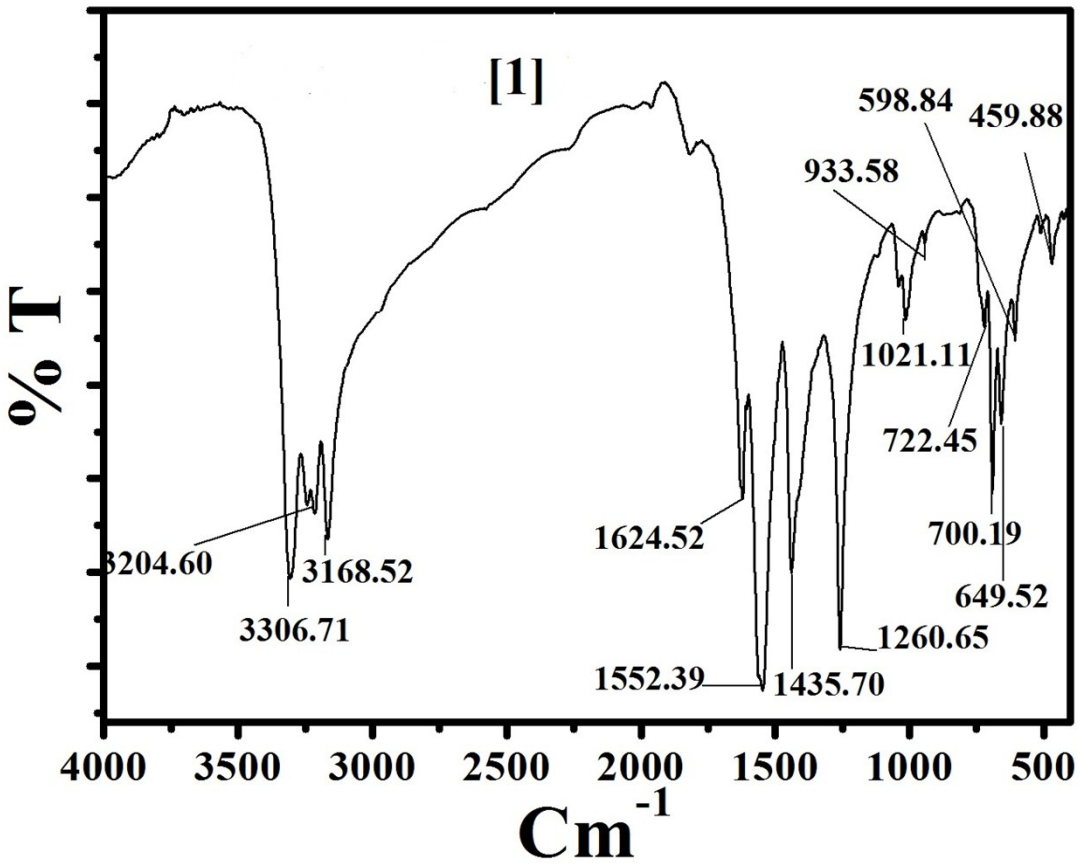

Figure S1. Infrared spectrum of **1**.

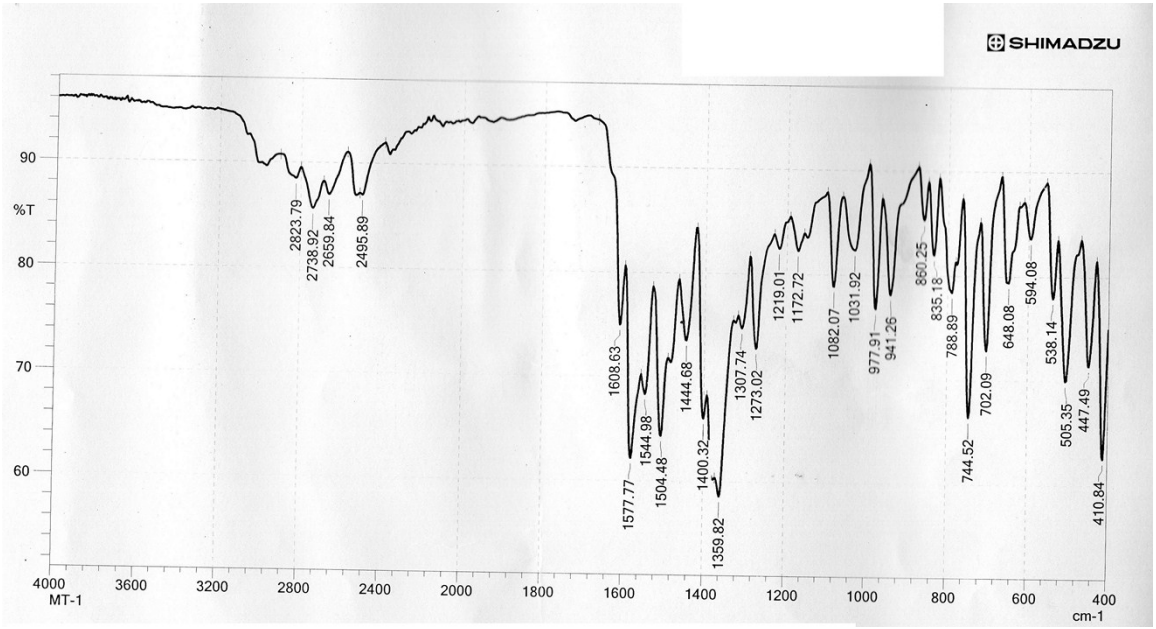

Figure S2. Infrared spectrum of **2**.

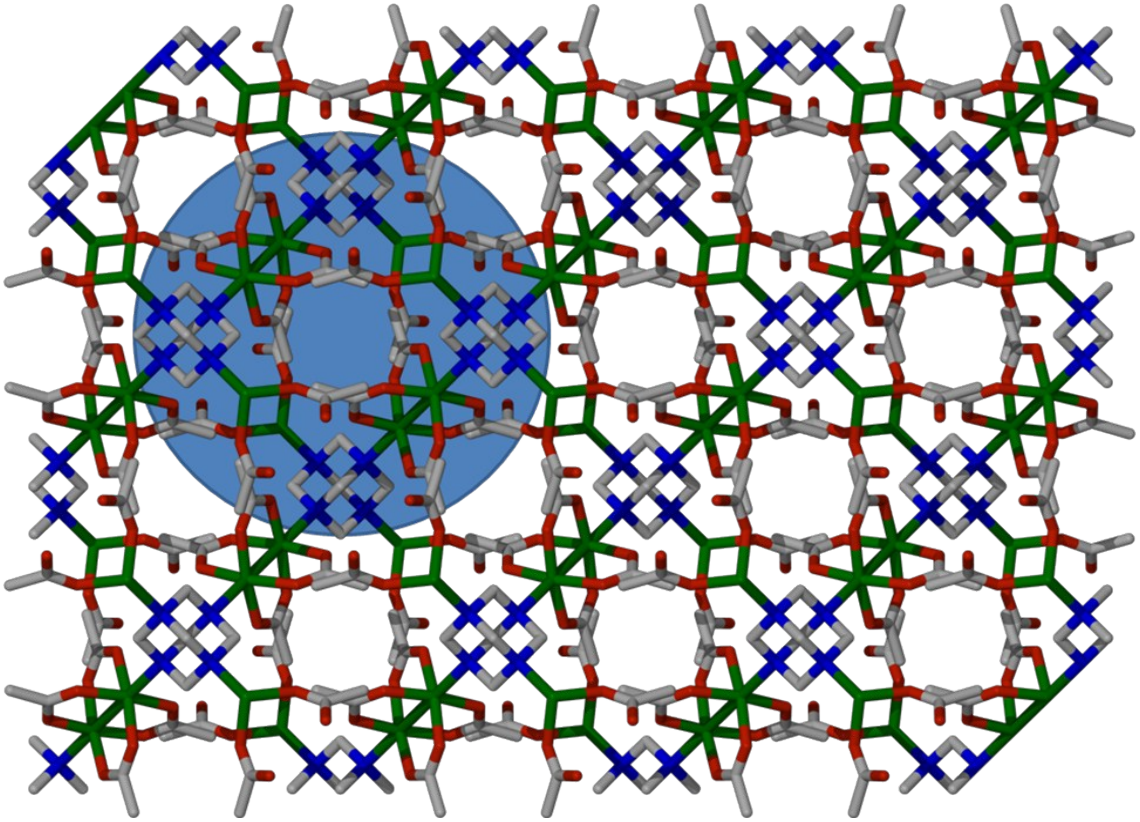

Figure S3. Six-membered ring in compound **1**.

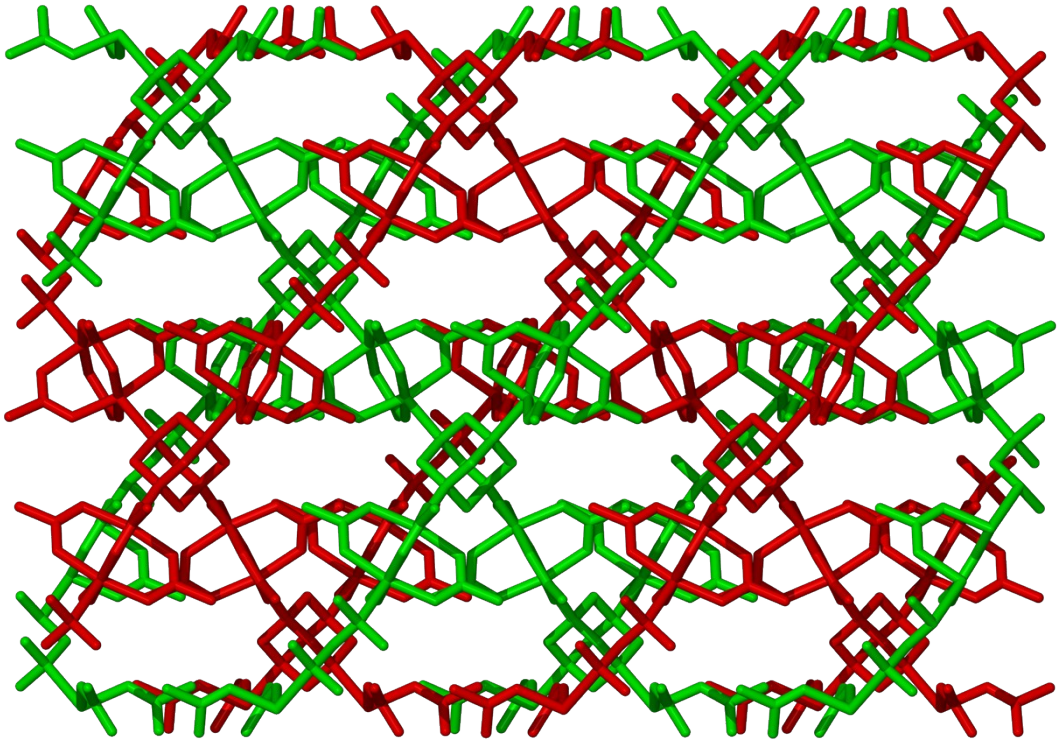

Figure S4. 2-fold interpenetrated network in **1**.

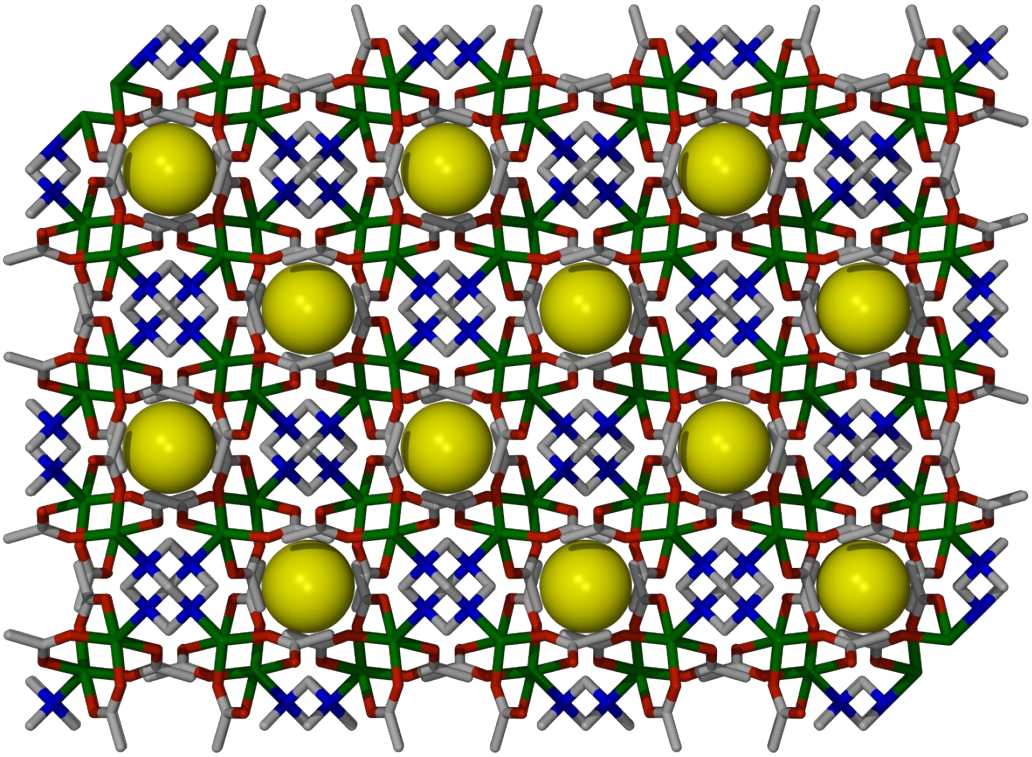

Figure S5. Channels formed along *c*-axis in **1**.

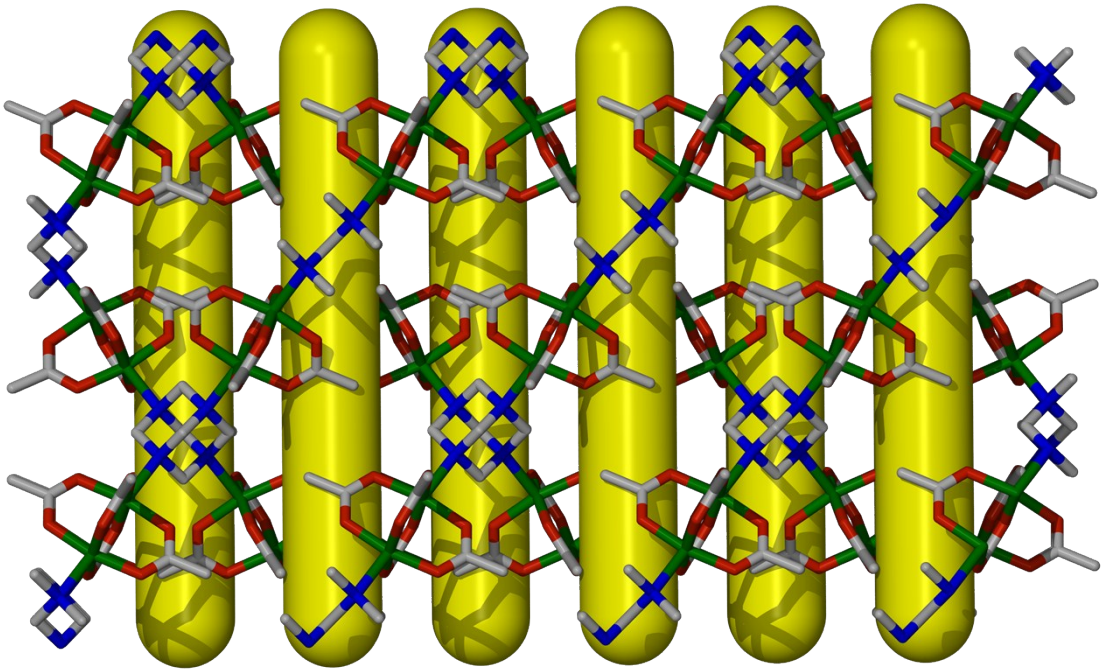

Figure S6. Displaying pores in the two-fold interpenetrated network of **1**. Yellow rods indicate the empty channels in **1**.

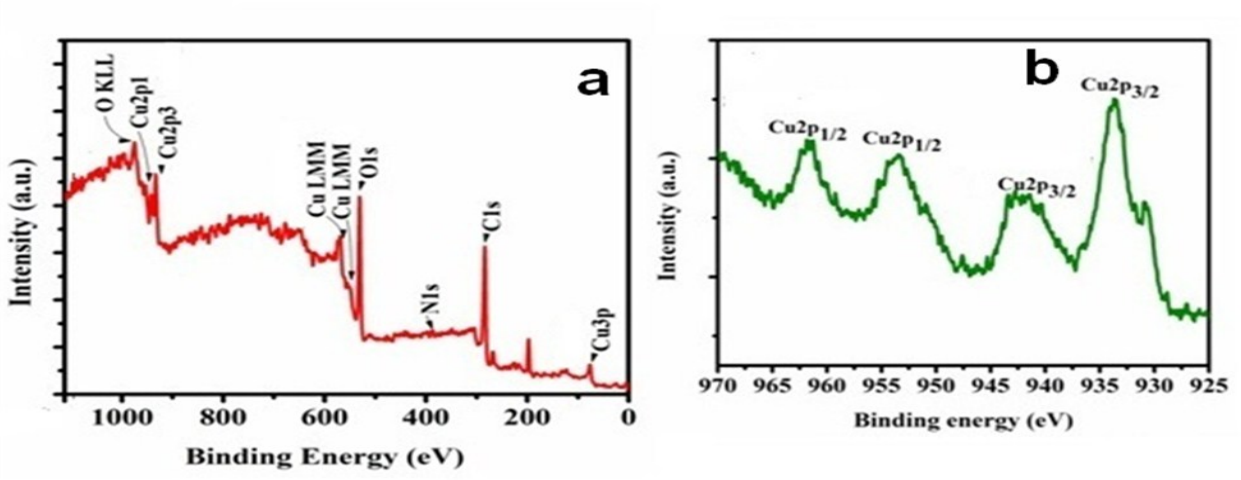

Figure S7. XPS spectra of compound **1** showing wide scan spectrum (a) and binding energies of Cu2p (b).

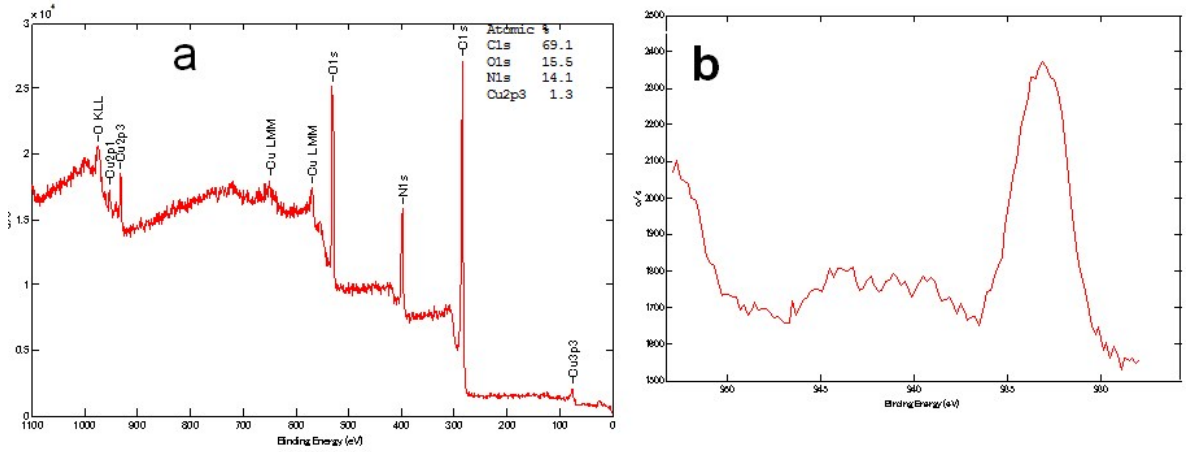

Figure S8. XPS spectra of compound **2** showing wide scan spectrum (a) and binding energies of Cu2p (b).

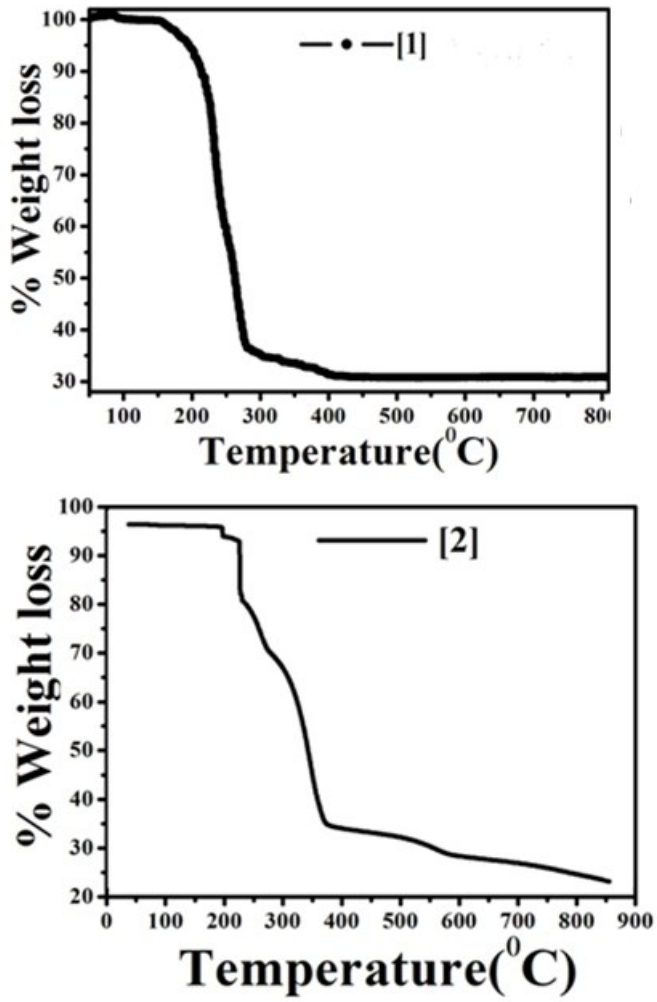

Figure S9. TGA profiles of $[Cu_2(OAc)_4(\mu_4\text{-hmt})_{0.5}]_n$ (**1**), and $[Cu\{C_6H_4(COO^-)_2\}_2]_n.2C_9H_{14}N_3$ (**2**) recorded under nitrogen flow.

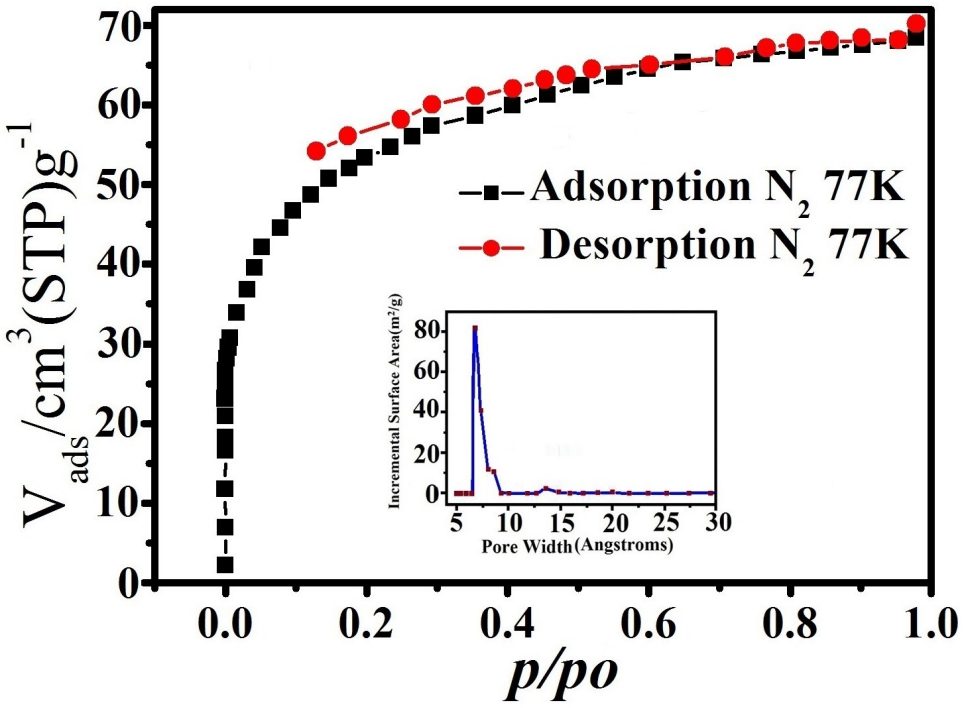

Figure S10. N_2 adsorption and desorption isotherm at 77K and pore size distribution (inset) of **1**.

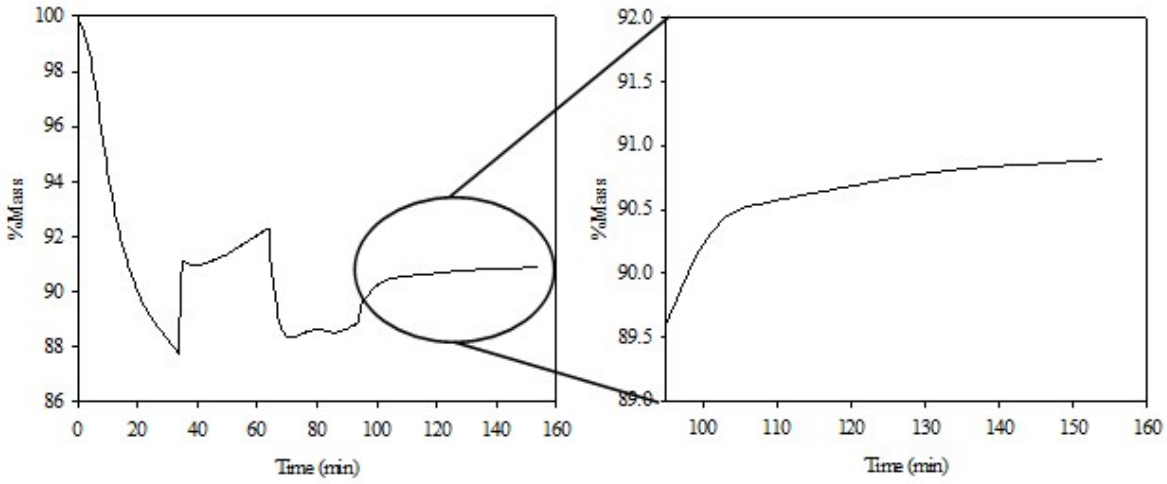

Figure S11. Kinetic studies for CO_2 capture (i) temperature profile, (ii) Compound **1**.

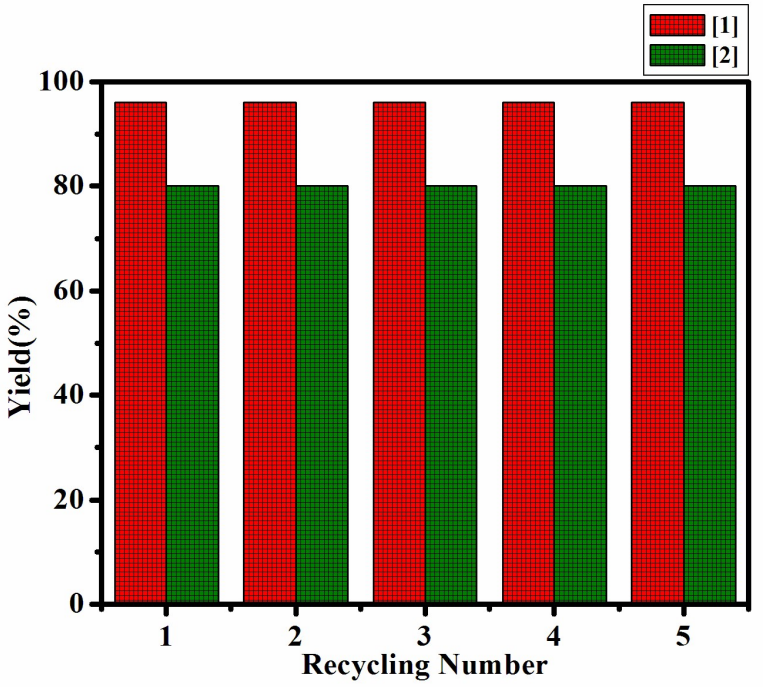

Figure S12. Histogram of recyclability study (five cycles) for catalytic activities of coordination polymers **1**, and **2** in coupling of glycidol with CO_2.

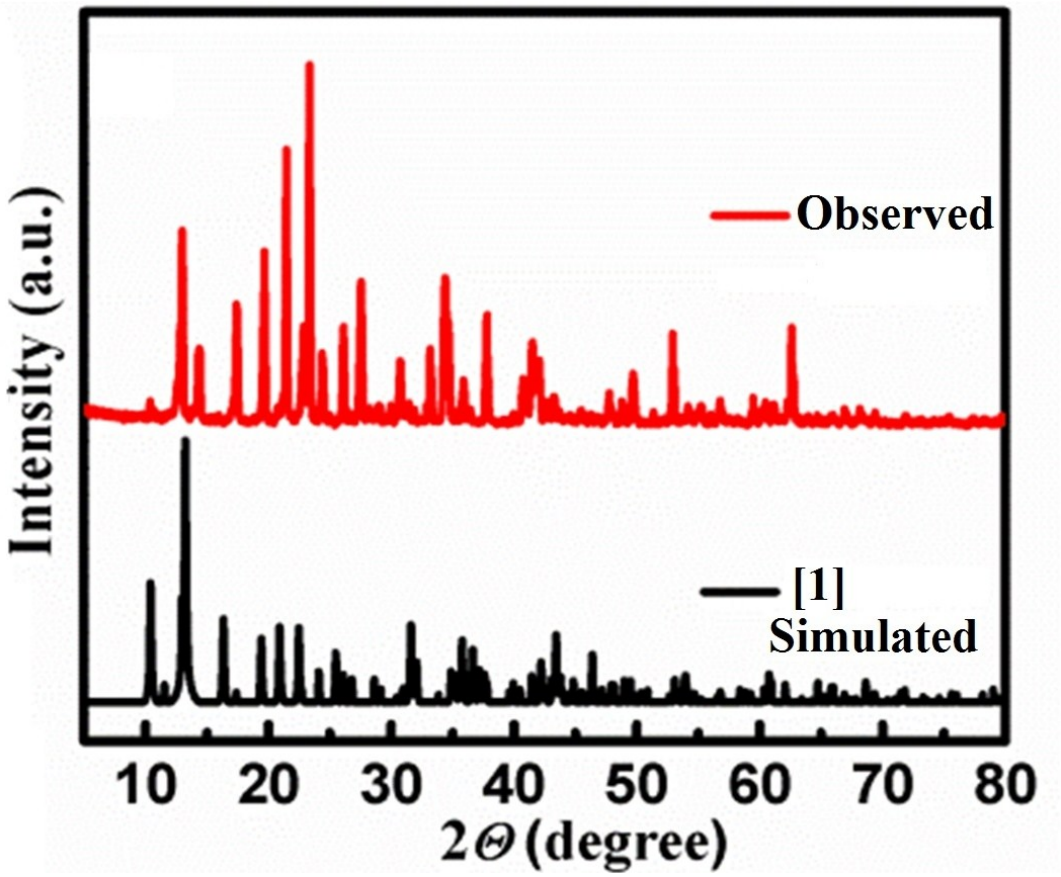

Figure S13. Powder XRD pattern of **1** after the catalytic reaction for coupling of glycidol with CO_2. (Simulated = theoretical profile based on the structures determined by single-crystal XRD; Observed= experimental data).

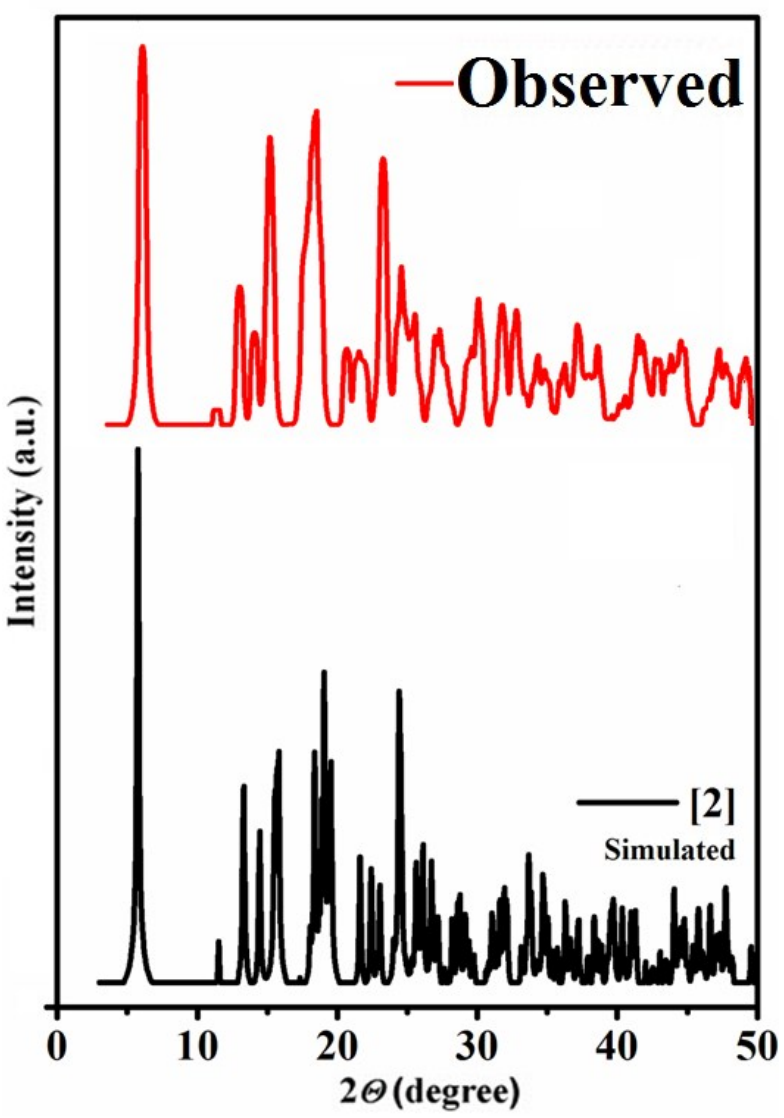

Figure S14. Powder XRD pattern of **2** after the catalytic reaction for coupling of glycidol with CO_2. (Simulated = theoretical profile based on the structures determined by single-crystal XRD; Observed= experimental data).

4-methyl-1, 3-dioxolan-2-one:

^{1}H NMR (400 MHz, $CDCl_3$): δ 1.49 (d, J=6.8 Hz, 3H), 4.06 (t, J=4.5 Hz, 1H), 4.73 (t, J=8.4 Hz, 1H), 4.86-4.93 (m, 1H); ^{13}C NMR (400 MHz, $CDCl_3$): 19.15, 70.53, 73.48, 154.95; GC-MS (EI) m/z (%):102 (M^+, 100).

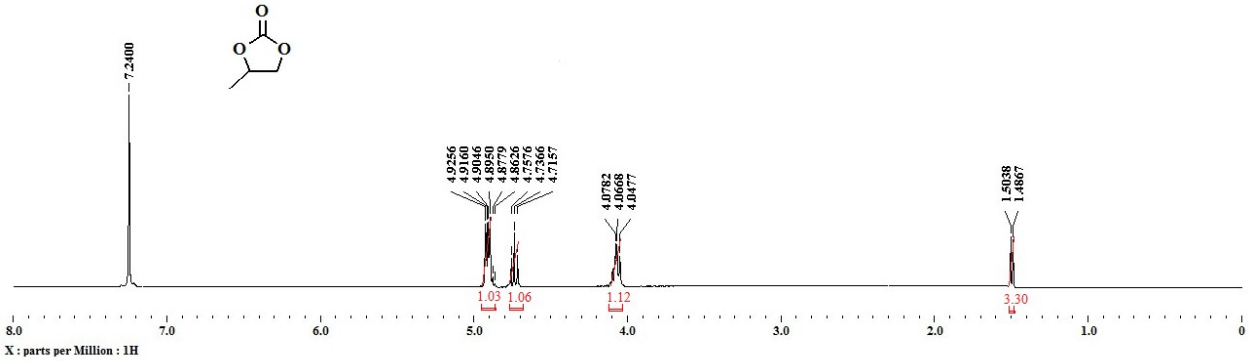

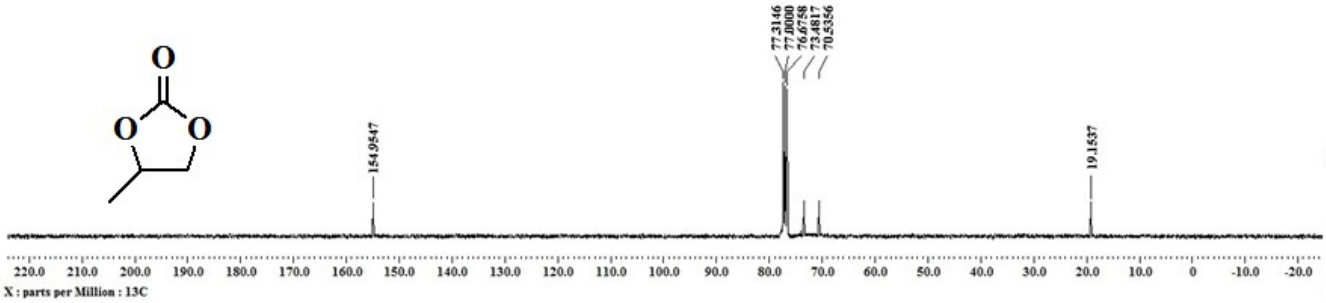

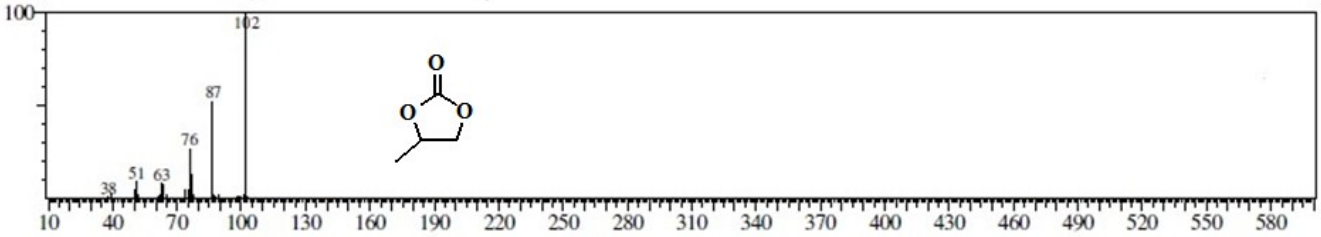

4-ethyl-1, 3-dioxolan-2-one:

^{1}H NMR (400 MHz, $CDCl_3$): δ 1.04 (t, J=1.5Hz, 3H), 1.73-1.86 (m, 2H), 4.09 (t, J=8Hz, 1H), 4.53 (t, J=4.4Hz, 1H), 4.61 (q, J=3.6Hz, 1H) ; ^{13}C NMR (400 MHz, $CDCl_3$): 155.08, 76.40, 68.04, 26.67, 8.36; GC-MS (EI) m/z (%):116 (M^+, 100).

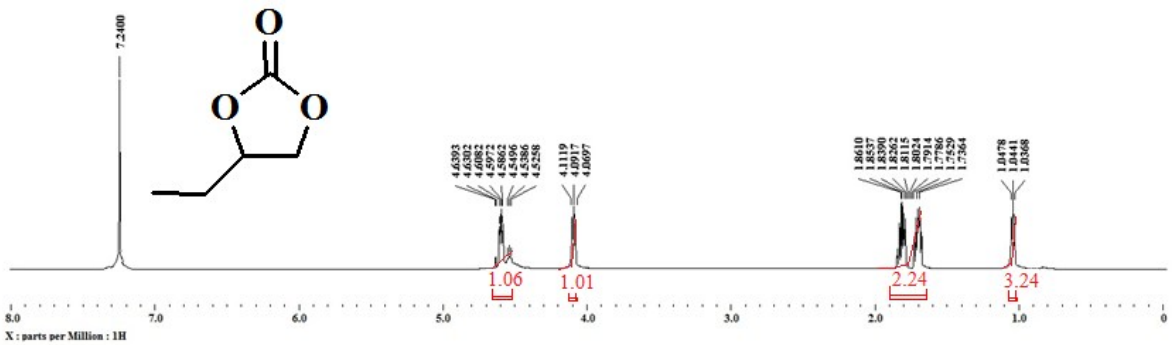

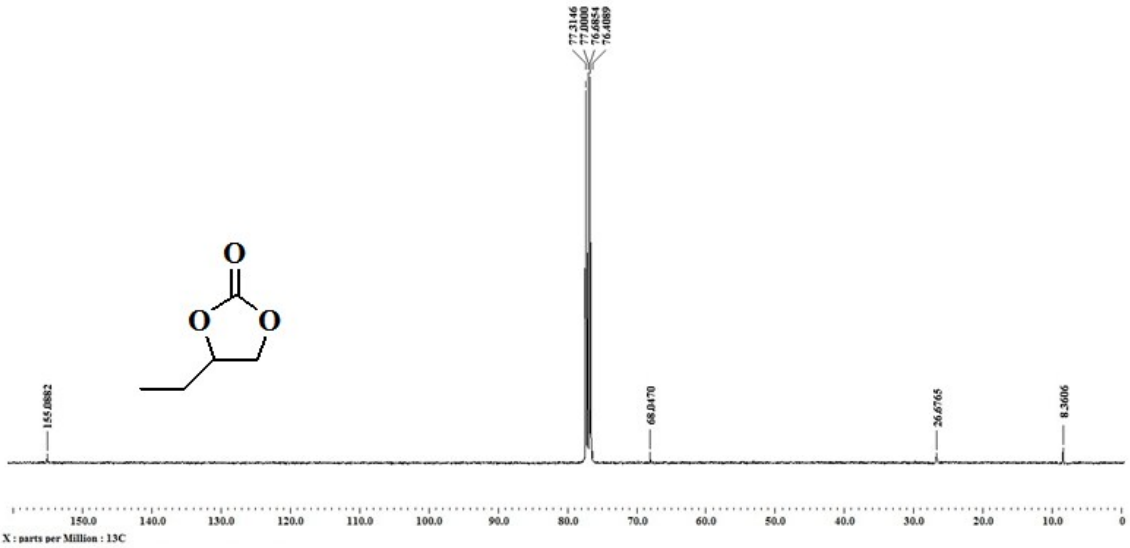

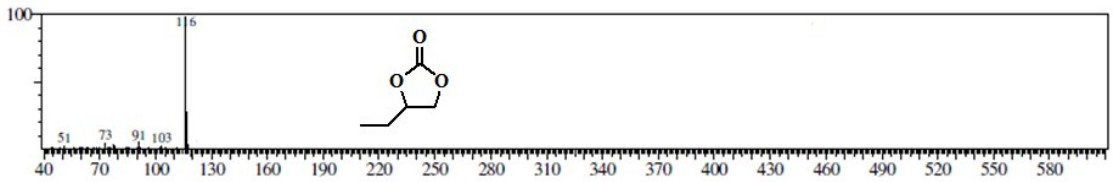

4-(chloromethyl)-1, 3-dioxolan-2-one:

^{1}H NMR (400 MHz, $CDCl_3$): δ 3.67-3.80 (m, 2H), 4.01 (dd, J = 3.6, 3.2 Hz, 1H), 4.58 (t, J = 1.0 Hz, 1H), 4.89-4.98 (m, 1H); ; ^{13}C NMR (400 MHz, $CDCl_3$): 43.83, 66.84, 75.48, 154.28; GC-MS (EI) m/z (%):137 (M^+, 100).

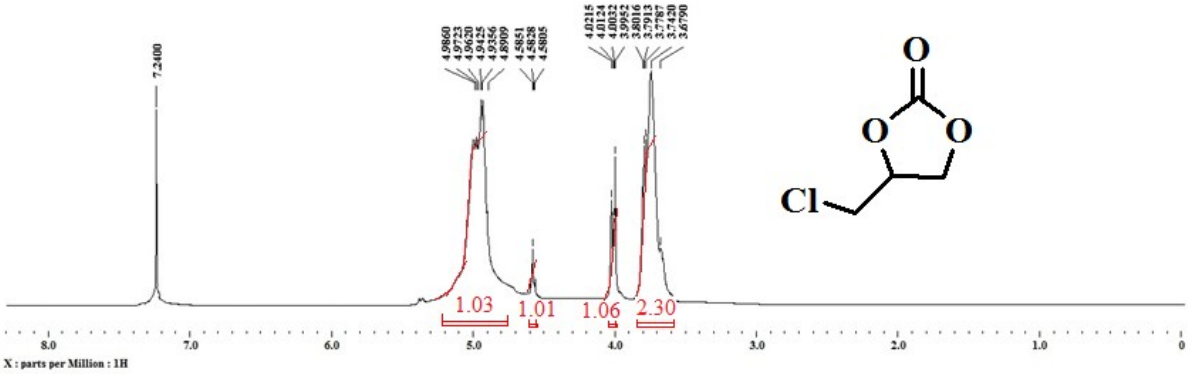

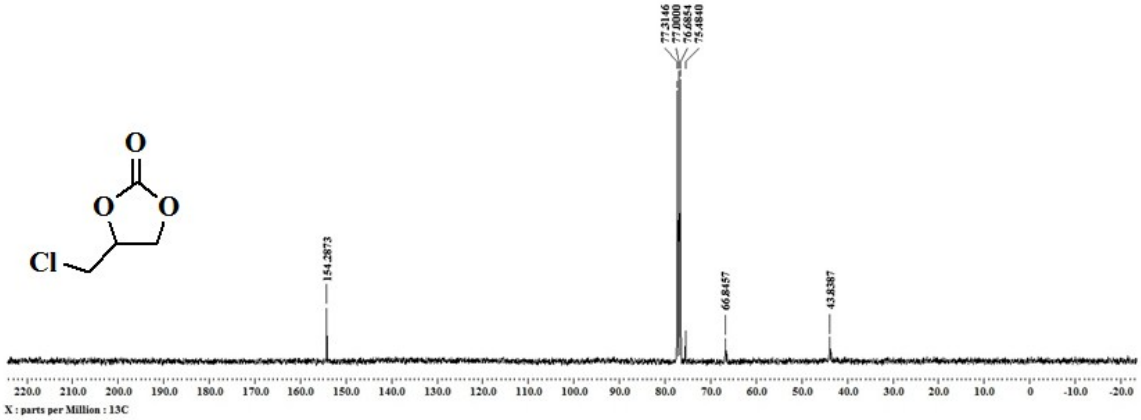

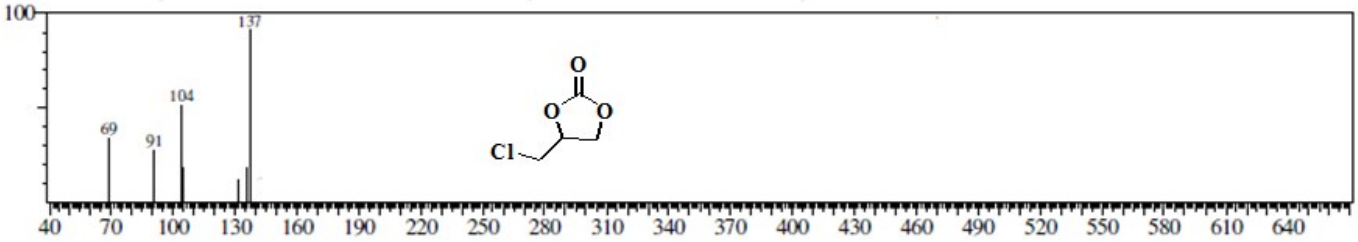

4-(bromomethyl)-1, 3-dioxolan-2-one:

^{1}H NMR (400 MHz, $CDCl_3$): δ 3.45-3.52 (m, 2H), 4.27-4.35 (dd, J = 13.7, 7.3 Hz, 1H), 4.58 (t, J = 1.0 Hz, 1H), 4.86-4.88 (m, 1H); ; ^{13}C NMR (400 MHz, $CDCl_3$): 31.32, 68.05, 73.92, 154.09; GC-MS (EI) m/z (%):181 (M^+, 100).

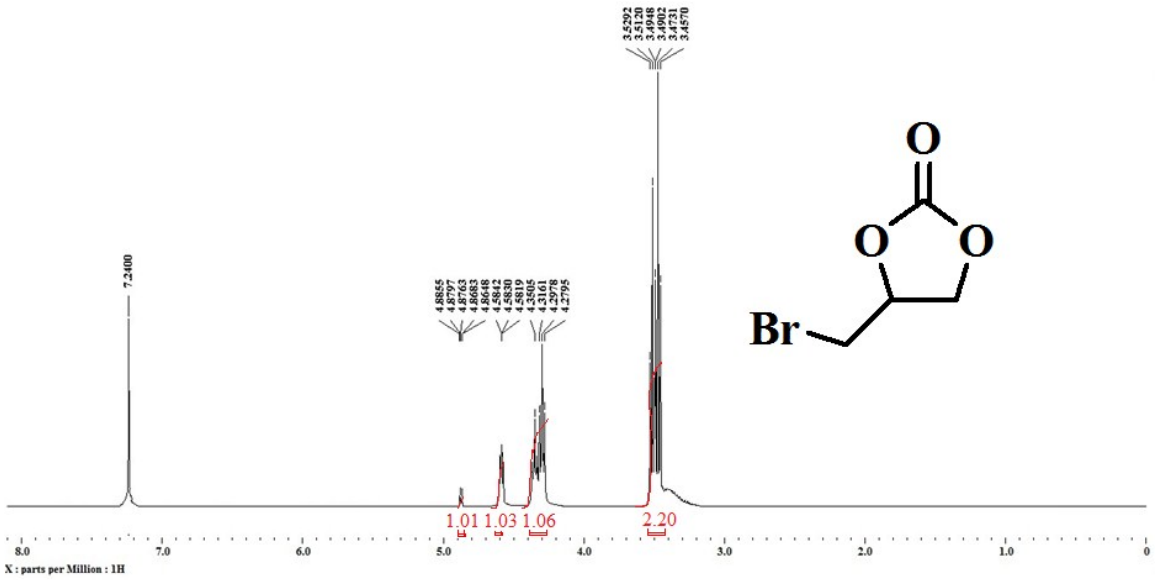

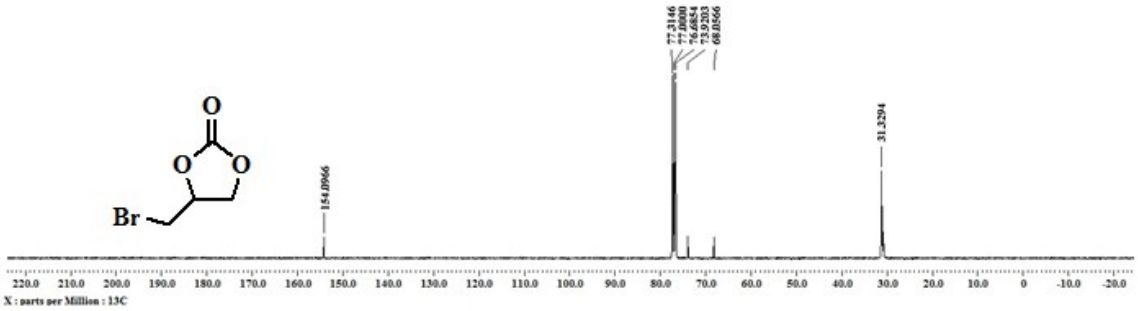

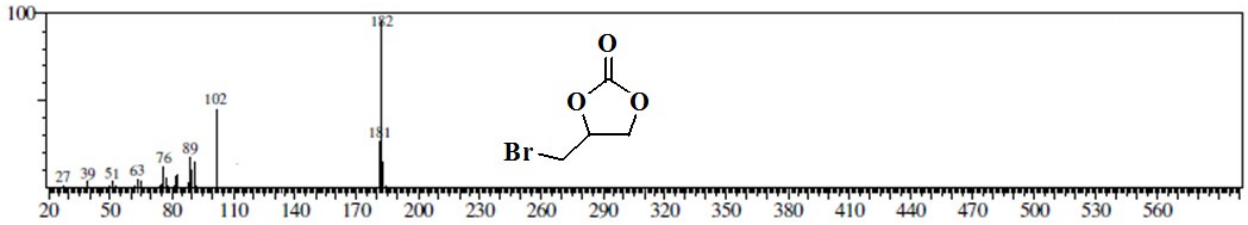

4-(hydroxymethyl)-1,3-dioxolan-2-one:

^{1}H NMR (400 MHz, $CDCl_3$): δ 4.80-4.82 (m, 1H), 4.14-4.21 (m, 2H), 4.01-4.02 (m, 1H), 3.30-3.58 (m, 1H), 2.45-2.50 (m, 1H); ^{13}C NMR (400 MHz, $CDCl_3$): 38.87, 39.08, 39.29, 39.50, 39.91, 40.41 , 60.61, 65.88, 155.20; GC-MS (EI) m/z (%):118 (M^+, 100).